Available online at www.sciencedirect.com
ScienceDirect
Physica E 40 (2008) 1586–1589
PHYSICA E
www.elsevier.com/locate/physe

Measurement of linear and cubic spin–orbit coupling parameters in AlGaN/AlN/GaN heterostructures with a polarization-induced two-dimensional electron gas

H. Cheng[a,*], N. Biyikli[b], Ü. Özgür[b], Ç. Kurdak[a], H. Morkoç[b], V.I. Litvinov[c]

[a]*Randall Lab, Physics Department, University of Michigan, Ann Arbor, MI 48109, USA*
[b]*Department of Electrical Engineering, Virginia Commonwealth University, Richmond, VA 23284, USA*
[c]*WaveBand/Sierra Nevada Corporation, 15245 Alton Parkway, Suite 100 Irvine, CA 92618, USA*

Available online 11 October 2007

Abstract

Spin–orbit coupling is investigated by magneto-conductivity measurements in $Al_xGa_{1-x}N/AlN/GaN$ heterostructures with a polarization-induced two-dimensional electron gas having a carrier density range from $0.8\times10^{12}\,cm^{-2}$ to $10.6\times10^{12}\,cm^{-2}$. The zero-field electron spin-splitting energies extracted from the weak antilocalization measurements are found to scale with the Fermi wavevector k_F as $2(\alpha k_F+\gamma k_F^3)$ with effective linear and cubic spin–orbit parameters of $\alpha=5.0\pm0.3\times10^{-13}\,eV\,m^3$ and $\gamma=1.6\pm0.6\times10^{-31}\,eV\,m^3$, respectively. The cubic spin–orbit coupling parameter is purely due to the bulk inversion asymmetry of the wurtzite crystal and has not been previously measured for the GaN system.

PACS: 73.20.Fz; 73.40.Kp; 71.70.Ej

Keywords: GaN; Spin–orbit coupling; Heterostructure; Spintronics; Two-dimensional electron gas

Following the prediction of above room temperature ferromagnetism in GaN-based dilute magnetic semiconductors [1], the GaN-based layer system emerged as very interesting candidates for spintronic applications [2]. However, for realization of useful spintronic devices based on GaN, several important physical processes such as generation, transport, and detection of spin must be performed in a controllable manner. These are challenging tasks, since spin is not a conserved quantity in semiconductor heterostructures. One of the important issues is the spin–orbit interaction in two-dimensional (2D) electron systems. Spin–orbit interaction is responsible for the spin relaxation in low dimensional semiconductor systems. In this context, it is essential to understand the spin–orbit coupling and the associated zero-field electron spin-splitting in GaN-based 2D electron systems.

It is well known that the spin-splitting for a 2D electron system originates from both the structural inversion asymmetry (SIA), i.e. Rashba term, of a quantum well (QW) [3] as well as the bulk inversion asymmetry (BIA) of the crystal [4,5]. The spin-splitting in GaN/AlGaN arising from the SIA scales linearly with the Fermi wavevector k_F, whereas there are two terms associated with BIA effect for a wurtzite structure: one scales as k_F and the other scales as k_F^3 and is anisotropic in the plane of GaN/AlGaN QW [6,7]. The Rashba coupling is of particular interest for gate controlled spin transistor applications [2] and the k_F linear BIA spin–orbit term is only specific to wurtzite (W) bulk crystals and does not exist in zinc-blende (ZB) structures. However, in a *c*-axis-oriented W-structure 2D system, both SIA and BIA effects have the similar terms in the effective spin–orbit coupling Hamiltonians [3]. The contributions of these terms have not been measured independently for the GaN/AlGaN heterostructures. Therefore, it remains a challenging task to differentiate the contributions by SIA and BIA effects in W-structure materials. Recently,

*Corresponding author. Tel.: +1 734 615 0195; fax: +1 734 763 9694.
E-mail address: hailing_cheng@hotmail.com (H. Cheng).

1386-9477/$ - see front matter © 2007 Elsevier B.V. All rights reserved.
doi:10.1016/j.physe.2007.09.184

zero-field spin–orbit splitting parameter has been calculated theoretically in wurtzite GaN/AlGaN heterostructures and a large spin–orbit coupling is predicted due to strong polarization field at the interface and polarization-induced doping [8,9]. However, in Ref. [9], the BIA coupling coefficients in III-nitrides were estimated from parameters of other semiconductor materials and only the effective linear coupling coefficient was obtained. The BIA terms were expected to be larger than SIA term in III-nitride QW [9]; that means the effective cubic BIA term scaling with k_F^3 is not negligible in W–GaN QW systems, especially when the carrier density is high. Furthermore, there have been conflicting reports on the size of spin-splitting energies based on the beat patterns of Shubnikov-de Haas (SdH) oscillations [10,11]. To resolve these issues, two other groups and we have recently used weak antilocalization (WAL) measurements to extract spin-splitting energies instead [6,7,12]. WAL measurements, which are reliable for studying the spin–orbit coupling, have been consistent among the aforementioned efforts and revealed that the spin splitting energies scale linearly with k_F at low carrier densities. In this work, we extended the WAL measurements to higher carrier densities and report the contribution of the cubic k_F^3 term due to the BIA effect for the first time.

We use $Al_xGa_{1-x}N$/AlN/GaN heterostructures with a wide range of carrier densities in this work. The heterostructures were all grown by metalorganic vapor-phase epitaxy on *c*-plane sapphire substrates and consist of the following layers: a 3 μm GaN buffer layer, a 1 nm AlN interfacial layer, a 25 nm $Al_xGa_{1-x}N$ layer and a 3 nm GaN cap layer where the Al composition x ranged from 0.1 to 0.35. All layers were undoped and the 2D electron gas (2DEG) is induced by spontaneous and piezoelectric polarization effects just below the AlN interfacial layer, which was used to suppress alloy scattering [13]. To study the magnetotransport properties 600 μm long × 100 μm Hall bar structures were fabricated by photolithography followed by dry etching. Ti/Al/Ti/Au contacts annealed at 900 °C were then used to form ohmic contacts to the 2DEG. The Hall bar samples A, B, C, D, and E were fabricated using heterostructures with Al compositions $x = 0.1$, 0.15, 0.25, 0.3, and 0.35, respectively. We also fabricated a gated Hall bar structure, sample F, which is identical to sample E except a metal gate was deposited on the heterostructure to vary the carrier density of 2D electrons.

The samples are characterized by magneto-resistance and Hall measurements in a variable temperature cryostat with a base temperature of 1.6 K. The carrier densities extracted from Hall and SdH oscillations were in agreement with each other. By employing the persistent photoconductivity effect in samples A–E [14], we were able to vary the carrier density of the samples in a controllable manner over the ranges of 0.8–1.3 × $10^{12}\,cm^{-2}$, 1.7–4.9 × $10^{12}\,cm^{-2}$, 3.1–6.7 × $10^{12}\,cm^{-2}$, 5.3–8.9 × $10^{12}\,cm^{-2}$ and 8.1–10.6 × $10^{12}\,cm^{-2}$ for the five heterostructures, respectively [7], at 1.8 K. In sample F, by applying a gate voltage from −1900 to 300 mV we were able to cover a carrier density range of 9.3–10.6 × $10^{12}\,cm^{-2}$. As expected, the sample with the highest Al concentration $x = 0.35$ exhibited the highest carrier density. In terms of mobility, sample B with the Al concentration of $x = 0.15$ had the highest electron mobility of $\mu = 20,\ 300\,cm^2/V\,s$ at a carrier concentration of $n = 4.9 \times 10^{12}\,cm^{-2}$ at 4.2 K [7].

To extract the spin–orbit coupling and the associated spin-splitting energies, we measured the quantum corrections to conductance at low magnetic fields. Typical traces of magneto-conductivity after the subtraction of the zero-field background, $\Delta\sigma = \sigma(B) - \sigma(0)$, obtained from two samples are shown in Fig. 1(a–b). There is a clear WAL behavior at magnetic fields below 2 mT at 1.8 K. This feature arises from the quantum interference of spin-dephased paths and can be used to quantify spin–orbit coupling in semiconductors. The size of WAL feature is strongly temperature dependent and decreases with increasing temperature whereas the width of the peak does not vary with temperature.

We analyzed the WAL effect by using the Iordanskii, Lyanda-Geller, and Pikus (ILP) equations [15]. For each sample, we determined the elastic scattering time τ_{tr}, the diffusion constant $D = v_F^2\tau_{tr}/2$, and the characteristic transport field $B_{tr} = \hbar/4eD\tau_{tr}$ using the measured values of carrier density and mobility. A typical transport field B_{tr} is around 7 mT in our experiment. We fit the data with two adjustable parameters, the spin–orbit field $B_{SO} = \hbar/4eD\tau_{SO}$ and the phase coherence field $B_\phi = \hbar/4eD\tau_\phi$, where τ_{SO} and τ_ϕ are the spin–orbit and phase coherence times, respectively. For the traces shown in Fig. 1(a–b), best fits are obtained using $B_{SO} = 1.81$ and 2.17 mT and $B_\phi = 0.095$ and 0.133 mT, for samples B and E, respectively.

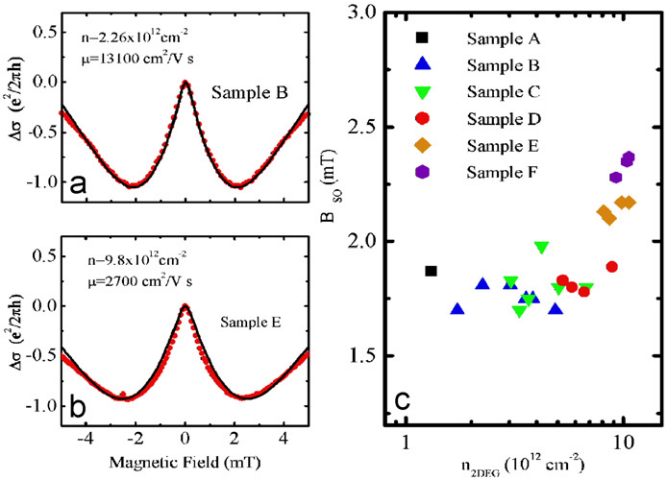

Fig. 1. (a–b) Magneto-conductivity after the subtraction of the zero-field background of samples B and E at $T = 1.6$ K. The solid lines are theoretical fits to the data. (c) B_{SO} extracted from WAL fits versus carrier density for six samples.

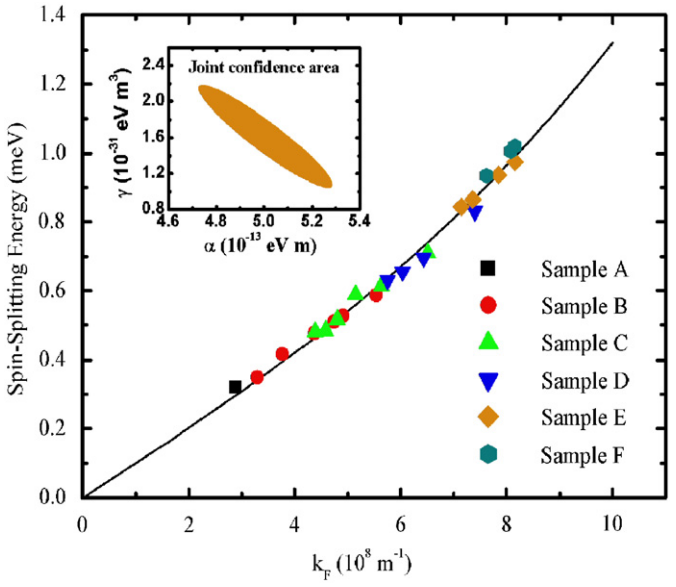

Fig. 2. The spin-splitting energy extracted from WAL measurements versus Fermi wavevector. The solid line is a fit to the data, which includes both the linear and cubic terms for spin–orbit interaction. The inset shows the 95% joint confidence area in the α–γ parameter.

In Fig. 1(c), we show B_{SO} versus the carrier density and a striking feature appears: as the carrier density varies from 1.7 to $10.6\times10^{12}\,\mathrm{cm}^{-2}$, B_{SO} varies from 1.7 to 2.37 mT. Since B_{SO} is proportional to the spin–orbit coupling parameter, this observation indicates that the spin–orbit energy is no longer a linear function of k_F at the particularly high carrier density. The spin-splitting energy $E_{SS}=2\hbar\Omega$ can be calculated from the spin–orbit field using the equation $B_{SO}=(\hbar/4eD)2\Omega^2\tau$, where Ω is the spin–orbit frequency. We plot the spin-splitting energies extracted from all the samples as a function of the Fermi wavevector k_F in Fig. 2. At low carrier densities, the spin-splitting energy is expected to scale linearly with k_F and at higher carrier densities there should be a crossover to the cubic region. A deviation from the linear behavior is evident in the data shown in Fig. 2. We should note that the Fermi wavevector is determined from the measured carrier density using $k_F=\sqrt{2\pi n}$, which assumes that the 2D electrons only occupy the lowest sublevel of the confinement potential. This assumption may no longer be valid at high carrier densities ($\sim10^{13}\,\mathrm{cm}^{-2}$) where the second subband would start to be occupied. Thus, the actual k_F would be a bit smaller than that given by the equation, in which case the deviation from the linear behavior observed in Fig. 2 would get even more enhanced. By fitting the data to a form $E_{SS}=2(\alpha k_F+\gamma k_F^3)$, we extracted the linear and cubic spin–orbit parameters of $\alpha=5.0\pm0.3\times10^{-13}\,\mathrm{eV\,m}$ and $\gamma=1.6\pm0.6\times10^{-31}\,\mathrm{eV\,m}^3$, respectively. This represents the first measurement of the cubic spin–orbit parameter for the GaN/AlGaN system. We also show in the inset in Fig. 2a 95% joint confidence area for the linear and cubic spin–orbit parameters based on a statistical error analysis of our data. The joint confidence area is a tilted ellipsoid in the α–γ parameter space; for the 95% confidence region it covers a range of 4.7–$5.3\times10^{-13}\,\mathrm{eV\,m}$ in α and 1.0–$2.2\times10^{-31}\,\mathrm{eV\,m}^3$ in γ.

For a W–$Al_xGa_{1-x}N$/AlN/GaN heterostructure, both the SIA of the QW (Rashba term) and the BIA of the crystal contribute to the linear term. We note that we did not observe any significant difference in the spin-splitting energies for sample E and F, where the carrier density was varied by the persistent photoconductivity effect and by gating, respectively. This suggests that the spin–orbit coupling cannot be varied easily by gating in this material system. Further theoretical and experimental work is needed to quantify the individual contributions of BIA and SIA to the linear term. In contrast, the cubic spin–orbit parameter purely arises from the BIA of the crystal. We note that the cubic parameter of GaN extracted from our measurements is 2 orders of magnitude smaller than that of GaAs [16].

In conclusion, we have extended WAL measurements of spin–orbit coupling in AlGaN/AlN/GaN 2D electron systems to carrier densities as high as $10.6\times10^{12}\,\mathrm{cm}^{-2}$. We find that the electron spin-splitting energies do not scale linearly with k_F at high carrier densities. From this deviation, we are able to extract the cubic spin–orbit parameter $\gamma=1.6\pm0.6\times10^{-31}\,\mathrm{eV\,m}^3$ for this material system for the first time, which suggest that the k_F^3 term from BIA effect in spin-splitting energy is not negligible in the high carrier density region.

We would like to thank Dr. V. Avrutin for useful discussions. This work is supported by grants from the Air Force Office of Scientific Research (AFOSR) under the direction of Dr. G.L. Witt and Dr. K. Reinhart, by the Missile Defence Agency Contract W9113M-04-C-0088 to WaveBand Corporation, and also by the NSF through Grant no. DMR-0606039.

References

[1] T. Dietl, H. Ohno, F. Matsukura, J. Cibert, D. Ferrand, Science 287 (2000) 1019.
[2] S. Datta, B. Das, Appl. Phys. Lett. 56 (1990) 665.
[3] E.I. Rashba, Fiz. Tverd. Tela (Leningrad) 2 (1960) 1224 (Sov. Phys. Solid State 2 (1960) 1109).
[4] G. Dresselhaus, Phys. Rev. 100 (1955) 580.
[5] L.C. Lew Yan Voon, M. Willatzen, M. Cardona, N.E. Christensen, Phys. Rev. B 53 (1996) 10703.
[6] S. Schmult, M.J. Manfra, A. Punnoose, A.M. Sergent, K.W. Baldwin, R.J. Molnar, Phys. Rev. B 74 (2006) 033302.
[7] Ç. Kurdak, N. Biyikli, Ü. Özgür, H. Morkoç, V.I. Litvinov, Phys. Rev. B 74 (2006) 113308.
[8] V.I. Litvinov, Phys. Rev. B 68 (2003) 155314.
[9] V.I. Litvinov, Appl. Phys. Lett. 89 (2006) 222108.
[10] I. Lo, W.T. Wang, M.H. Gau, S.F. Tsay, J.C. Chiang, Phys. Rev. B. 72 (2005) 245329.
[11] N. Tang, B. Shen, M.J. Wang, Z.J. Yang, K. Xu, G.Y. Zhang, D.J. Chen, Y. Xia, Y. Shi, R. Zhang, Y.D. Zheng, Phys. Rev. B 73 (2006) 037301.

[12] N. Thillosen, S. Cabanas, N. Kaluza, V.A. Guzenko, H. Hartdegen, Th. Schapers, Phys. Rev. B 73 (2006) 241311(R).
[13] M. Miyoshi, H. Ishikawa, T. Egawa, K. Asai, M. Mouri, T. Shibata, M. Tanaka, O. Oda, Appl. Phys. Lett. 85 (2004) 1710.
[14] N. Biyikli, Ç. Kurdak, Ü. Özgür, X.F. Ni, Y. Fu, H. Morkoç, J. Appl. Phys. 100 (2006) 103702.
[15] S.V. Iordanskii, Y.B. Lyanda-Geller, G.E. Pikus, JETP Lett. 60 (1994) 207.
[16] P.D. Dresselhaus, C.M. Papavassiliou, R.G. Wheeler, Phys. Rev. Lett. 68 (1992) 106.